Journal of Chromatography, 648 (1993) 27–32
Elsevier Science Publishers B.V., Amsterdam

CHROMSYMP. 2823

Mean square radius of molecules and secondary instrumental broadening

Philip J. Wyatt

Wyatt Technology Corporation, 802 East Cota Street, P.O. Box 3003, Santa Barbara, CA 93130-3003 (USA)

ABSTRACT

In a chromatographic separation such as size-exclusion chromatography, the concentrations of the injected molecules are generally so low by the time they reach the light-scattering (LS) detector that terms involving the second virial coefficient may be neglected in the equations which relate the measured Rayleigh excess ratio to the derived molecular weights and sizes. For sufficiently large molecules (root mean square radius greater than about 10 nm for 633 nm incident light wavelength), the root mean square radius may be calculated independently of the molecular concentration from the Rayleigh ratios measured as a function of scattering angle. Precise measurements of the root mean square radius are presented for some nearly monodisperse polystyrene standards. These measurements confirm that the eluting molecules have a nearly constant size over a relatively broad range of elution volumes, yet the corresponding mass values are not constant. This inconsistency is shown to be due to a secondary instrumental broadening (IB) of the sample which occurs primarily in the refractive index detector which follows the LS detector. This secondary IB, which may be calculated from the distorted mass *versus* elution volume curves, is shown to vary with molecular mass.

Consider the following equation [1] which is based on the Rayleigh–Gans–Debye (RGD) approximation [2] in the limit of vanishingly small molecular concentrations, c, and which forms the basis for the interpretation of light scattering measurements made from solutions of macromolecules of weight-average molecular mass M_w.

$$\frac{K^*c}{R(\theta)} \approx \frac{1}{M_w P(\theta)} + 2A_2c \tag{1}$$

The left-hand side of eqn. 1 represents the quantities measured and the right-hand side includes the unknown quantities to be determined by means of a least squares fit to the experimental data. In particular, $R(\theta)$ is the excess Rayleigh ratio,

$$R(\theta) = f_{geom}[I(\theta) - I_S(\theta)]/I_0 \tag{2}$$

where $I(\theta)$ is the intensity of light scattered by the solution into the solid angle subtended by the detector at the scattering angle θ, $I_S(\theta)$ is the corresponding quantity for the pure solvent, I_0 is the incident intensity, and f_{geom} is an absolute calibration constant that is a function of the scattering geometry, the structure of the (scattering) cell containing the solution, and the refractive indices of the solvent and scattering cell. The physical constant K^* for vertically polarized incident light is given by

$$K^* = 4\pi^2(dn/dc)^2 n_0^2/(N_A\lambda_0^4) \tag{3}$$

where n_0 is the solvent refractive index, N_A is Avogadro's number, λ_0 is the vacuum wavelength of the incident light, and dn/dc is the refractive index increment. The second virial coefficient is A_2. The scattering function, $P(\theta)$, is a function of the half scattering angle $\theta/2$ and the mean square radius, $\langle r_g^2 \rangle$:

$$P(\theta) = 1 - \left(\frac{4\pi n_0 \sin\theta/2}{\lambda_0}\right)^2 \langle r_g^2 \rangle /3 + \alpha_2 \sin^4\theta/2 - \cdots \tag{4}$$

0021-9673/93/$06.00

where

$$\langle r_g^2 \rangle = \frac{1}{M} \int r^2 \, dm \qquad (5)$$

and α_2 and higher order coefficients [3,4] in this $\sin^2 \theta/2$ series are constants dependent on the structure of the molecules. Note that the integral of eqn. 5 is the *definition* of the mean square radius. The integration (or summation) is taken over all mass elements dm of a molecule of mass M at a distance r from the molecule's center of gravity. The mean square radius is not the same as the so-called hydrodynamic radius.

At the very low concentrations typical of high-performance size-exclusion chromatography (HPSEC), the determination of the mean square radius [5] from the recorded light scattering data as a function of angle is easily shown to be independent of the concentration, c, the refractive index increment, dn/dc, and the weight-average molecular mass, M_w. Note that at such low concentrations when $2M_w A_2 c << 1$, eqn. 1 reduces to the simple form

$$\frac{R(\theta)}{K^*} = McP(\theta), \qquad (6)$$

i.e. $P(\theta)$ is directly proportional to $R(\theta)$ and the results of ref. 5 follow. (This is true even for the case of heterogeneous co-polymers as long as only one molecular species is present in each detected eluting fraction. If more than a single species is present in any fraction, then they must all have approximately the same refractive index increment, dn/dc). Indeed, the mean square radius may always be determined even for elution regions where there is no differential refractive index (DRI) detector signal. All that is required is that the light scattering signals at the various detectors (angles) be sufficiently strong so that the coefficient of the term linear in $\sin^2 \theta/2$ of eqn. 4 may be determined [5].

Fig. 1 illustrates an excellent example of a strong light scattering signal without a corresponding DRI signal. In the foreground is the DRI signal (marked at the right with the small symbol *ri*) as a function of elution volume while the excess Rayleigh ratios, $R(\theta)$, at the different angles collected by the DAWN detector (Wyatt Technology Corporation, Santa Barbara, CA, USA), are shown behind, also as a function of elution volume. The sample was comprised of a set of biopolymers (in an aqueous buffered solution) used for calibration purposes in HPSEC measurements. At the smallest elution is seen the light scattering signature of a very large aggregate which produces no DRI signal. The z-average root mean square radius for this peak is over 64 nm and easily calculated independently of the concentration, dn/dc, and M_w values.

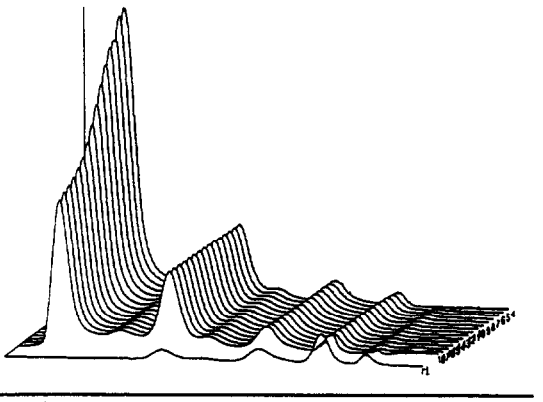

Fig. 1. Rayleigh excess ratio as a function of scattering angle (detector) from a set of biopolymers showing the presence of a large aggregate whose corresponding DRI signal is negligible. This fraction, which yields a very intense and steep variation of scattered light intensity, is shown at the smallest elution volume to the left of the figure.

A great number of papers have been written [6–10] concerning so-called band broadening or instrumental broadening (IB) effects and the corrections to the measured data required to recover the correct mass distribution present in the separated sample. Although by far the greatest broadening occurs within the columns, a smaller, secondary broadening may occur in the mass detector that follows them. With a light-scattering (LS) detector inserted between the columns and the mass detector, the broadening that occurs within the column will not affect the derived weight-average molecular masses as long as the concentration at each eluting slice is known as it reaches the LS detector. Unfortunately, the concentration variation itself may be distorted by the secondary instrumental broadening that occurs *after* the LS detector.

The slight distortions in concentration profiles

that are due to the large DRI dead volumes, tubing mismatches, and other flaws in the subsequent chromatographic are rarely important when measuring polymers of relatively broad distribution. Such secondary distortions, however, become very important for extremely narrow standards such as those used frequently for system calibration for conventional HPSEC. Perhaps of more immediate importance are protein applications where even the slightest instrumental band broadening can yield unreasonable molecular distributions for species known to be monodisperse.

What has been developed here is the ability to measure the secondary IB effects *directly* without disturbing the measurement by introducing an additional detector. It may be reasoned that the secondary broadening caused by a DRI detector may be measured easily by placing two such detectors in sequence. Such an arrangement permits only a determination of the *difference* of the DRI response profile which, in turn, requires a somewhat complex deconvolution to extract the functional form of the net broadening of a single detector. Most DRI detectors, furthermore, have very large diameter tubing after their detection cell (to reduce back pressure) which would affect secondary IB were it not (usually) the last element of the HPSEC system. Using very narrow standards whose root mean square radii are accurately measurable, a light scattering detector can be used to determine most of the broadening of the sample that occurs in the region between the columns and the end of the DRI detector cell, as will be shown presently. For the measurements reported here, only about 17% of the volume contributing to the secondary IB is in the LS detector itself. This will have a small effect on the derived secondary IB which is due primarily to the large volume of tubing often required by the DRI detector to maintain thermal stability.

Fig. 2 presents the excess Rayleigh ratio as a function of detector (angle) measured with a DAWN light scattering detector ($\lambda = 632.8$ nm) from a sample of three polystyrene standards (Pressure Chemical Co., Pittsburgh, PA, USA; lot numbers 30121, 50912 and 80317) separated using two mixed-bed Shodex (Showa Denko, Tokyo, Japan) KF 80M columns at a tetrahydrofuran flow-rate of 1.0 ml/min. Shown in the foreground is the RI signal from a Waters 410 detector, suitably corrected for a volume delay of 173 ml. (This delay volume is made up of approximately 30 μl from DAWN instrument, 11 μl from the tubing connecting the DAWN to the Waters 410 and a dead volume in the Waters 410 from the inlet to the end of the DRI cell of 133 μl. Although the actual cell volume of the Waters 410 is given by the manufacturer as 56 μl, a large tubing dead volume is needed to assure good temperature stability, especially at high flow-rates.) The signals from some detectors have been dropped because of noise. Fig. 3

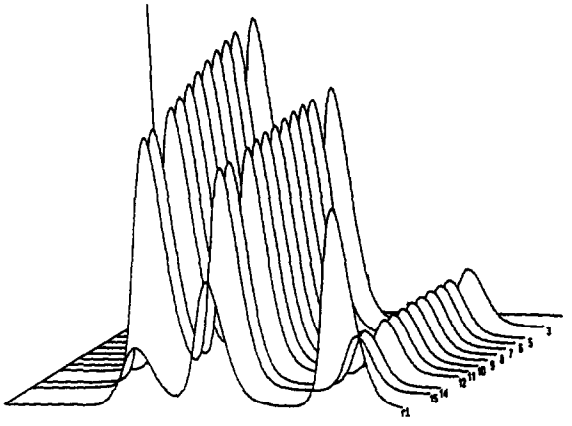

Fig. 2. Rayleigh excess ratio as a function of scattering angle (detector) from three polystyrene standards and contrasted with the corresponding signal from the RI detector, shown in the foreground.

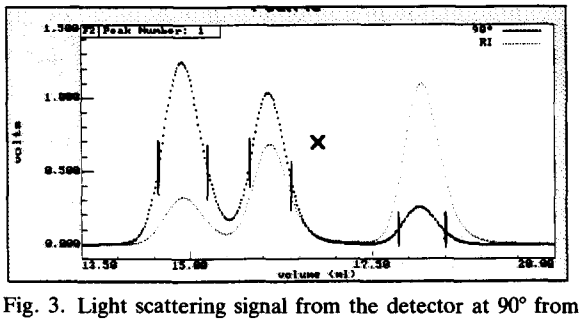

Fig. 3. Light scattering signal from the detector at 90° from Fig. 1 overlaid with the signal from the DRI detector and corrected for the delay volume between the DRI and DAWN instruments. The central region of each peak corresponding approximately to the full width at half maximum is indicated by each pair of vertical bars.

shows the 90° light-scattering signal (DAWN detector 11) overlaid with the DRI signal which is corrected for the 173-μl delay volume. The central regions of each peak, defined approximately as the peak full width at half maximum, are clearly indicated by the vertical bars. The three corresponding weight average molecular masses for these regions as marked are 606 000, 217 000 and 31 300, respectively. The corresponding masses mixed and injected in a 100-μl loop were $9.5 \cdot 10^{-2}$, $1.7 \cdot 10^{-1}$ and $2.7 \cdot 10^{-1}$ mg, respectively.

Table I presents the software (ASTRA, Wyatt) generated light-scattering characteristics of the three narrow regions delineated in Fig. 3. These include the number-, weight- and z-average molecular masses (M_n, M_w and M_z), the corresponding weighted root mean square radii r_{g-n}, r_{g-w} and r_{g-z} and finally the sample polydispersity defined as the ratio M_w/M_n. The columns used for the separation were not optimal as evident from the overlap seen in Fig. 3 between the two larger samples. Nevertheless, the small sample *fractions* delineated in Fig. 3 may have considerably smaller polydispersities than the corresponding *total* samples.

Fig. 4 shows the root mean square radius as a function of elution volume for the three regions selected. Note that for the smallest, 30 000, fraction, the size cannot be clearly derived since it is below the limits of resolution for the 632.8-nm laser wavelength used. Figs. 5 and 6 present, respectively, the corresponding mass variations for the two largest fractions based on calculation by eqn. 1 with the concentration profile generated by the inline DRI detector. Since the root mean square radii for these fractions are *constant*, the corresponding masses also *must be constant*. Thus any deviation from mass constancy must be due entirely to a distortion of the concentration profile at the DRI detector due to secondary broadening effects.

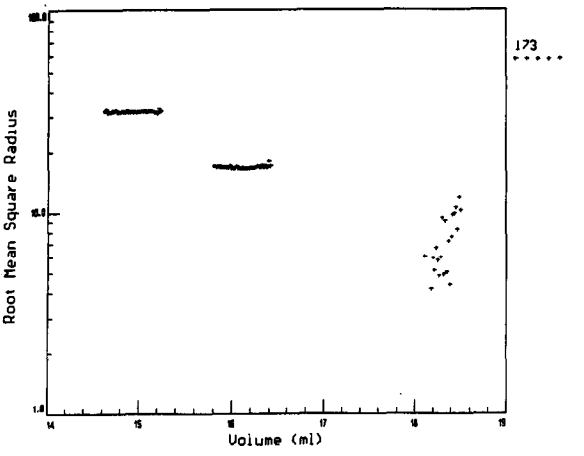

Fig. 4. Root mean square radius *versus* elution volume for the three regions indicated in Fig. 2.

If the weight-average molecular mass at a slice

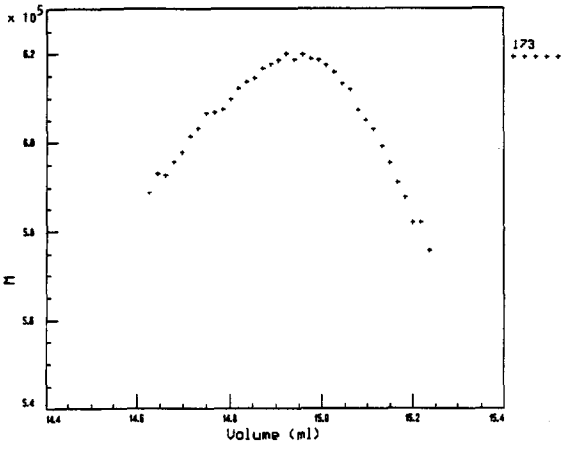

Fig. 5. Apparent mass variation with elution volume for the 606 000 fraction of Fig. 2.

TABLE I

MOLECULAR MOMENTS FROM LIGHT SCATTERING

Peak	M_n	M_w	M_z	r_{g-n}	r_{g-w}	r_{g-z}	M_w/M_n
1	605 870	606 120	606 360	31.7	31.7	31.7	1.0004
2	216 450	216 550	216 650	16.9	16.9	16.9	1.0005
3	31 271	31 297	31 321	6.9	6.9	6.9	1.0008

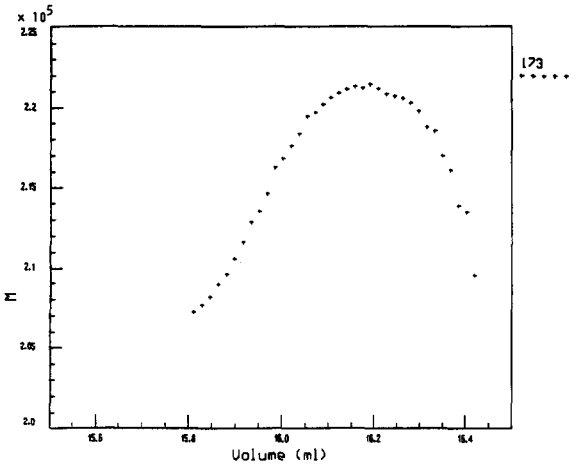

Fig. 6. Apparent mass variation with elution volume for the 217 000 fraction of Fig. 2.

i is given by M_i and the corresponding concentration is c_i, then we have immediately the relationship between the erroneously calculated mass M_i' and the secondary IB distorted concentration, c_i', as

$$\frac{M_i'}{M_i} = \frac{c_i}{c_i'} = \rho \tag{7}$$

However, since M_i must be constant ($=M$, say) at each slice in the region (since the $\langle r_g^2 \rangle$ values are constant), the corrected concentration c_i for each region where the eluting mass is constant is given simply by

$$c_i = \rho c_i' = c_i' M_i'/M \tag{8}$$

The weight-average molecular mass of the monodisperse sample, M_w, may be determined independently of the HPSEC-derived value (assumed to be slightly in error due to secondary IB) by performing an off-line Zimm [1] plot analysis of the unseparated sample. Thus the secondary instrumental broadening may be measured directly by means of effectively monodisperse standards whose root mean square radii may be determined accurately to be constant over a reasonable range of elution volumes. As pointed out for Gugliotta *et al.* [10] for the case of low-angle light scattering (a subset of the more general form discussed here), the response for a strictly monodisperse sample is proportional to the product of the concentration and molecular mass. Since the molecular mass is constant, the recorded concentration response is directly proportional to the standard spreading function, g(*t*), *i.e.*

$$g(t) \propto c_i' = c'(t) \tag{9}$$

Although Alba and Meira [11] state that truly monodisperse synthetic polymers are "... impossible to obtain ...", the measurements reported here of size monodispersity, confirm that for selected eluting regions, such monodispersity is small enough to permit the deduction of secondary IB. For example, even with the mass variations shown in Figs. 4 and 5, the corresponding polydispersities (M_w/M_n) are calculated to be 1.0004 and 1.0005, respectively. Introducing a constant mass for each of these fractions reduces the corresponding polydispersities to 1.0000 and 1.0001, respectively. The latter deviation from unity is due entirely to the slight experimental uncertainties. The apparently small uncorrected values have been discussed above.

Although no measure of the mean square radius of the smaller 31 300 fraction is possible, the calculated polydispersity shown in Table I suggests that it too may be quite monodisperse. On this basis, it is instructive to examine the dilution factors ρ for all three mass fractions as a function of $t - t_0$, where t_0 corresponds to the time at which the peak concentration is detected (in seconds) at the DRI detector. These are shown in the abbreviated Table II. (The data were collected every second and only every third point is shown. These data have been smoothed by replacing each value with a three-point average including the values of its two adjacent slices.) At a flow-rate of 1 ml/min, each second corresponds to approximately 16.7 μl. Some rather interesting observations may be made from these results. The dilution factors (secondary IB factors, ρ) are not symmetric (probably due to tailing effects in the intervening volumes); they are a function of molecular mass, but do not appear to vary monotonically with molecular mass; and this latter variation most probably depends on the geometry of the various

TABLE II

DILUTION FACTORS FOR THREE MASS FRACTIONS

$t - t_0$	$\rho_{606\,000}$	$\rho_{217\,000}$	$\rho_{31\,300}$
−15	0.9661	0.9584	0.9382
−12	0.9796	0.9619	0.9636
−9	0.9911	0.9727	0.9842
−6	1.0015	0.9870	0.9945
−3	1.0095	1.0016	1.0100
0	1.0167	1.0121	1.0137
3	1.0211	1.0189	1.0230
6	1.0212	1.0216	1.0247
9	1.0154	1.0215	1.0253
12	1.0032	1.0184	1.0204
15	0.9883	1.0115	1.0083
18	0.9681	0.9961	0.9905

"dead volumes" involved. It is important to stress further than the secondary IB effects measured here are *extremely* small; probably much smaller than might even be noticed since the polydispersities shown in Table I were calculated from the *uncorrected* data and these are in themselves far less than the values quoted by the manufacturer as "less than 1.06". The manufacturer's values are based on HPSEC calibrations and refer to the entire peaks, not just the small central regions selected in this paper. The extremely small secondary IB effects measured here augur well for the future, since much greater secondary IB effects are easily introduced by adding more dead volume introducing tubing of sharply varying crosssections, or permitting kinks or burrs within the tubing. The sensitivity of the technique is very great, though only applicable to molecules sufficiently large so that their mean square radii may be determined accurately.

The thesis proposed in this paper, that uniformity of the derived mean square radius allows one to conclude that the selected sample has a similarly monodisperse mass distribution should prove to be extremely important for examining explicitly the form of secondary instrumental broadening (without the introduction of any major assumptions) as a function of molecular mass, flow-rate, column structure, the volume delay between columns and detectors, and the dead volume of the detectors themselves. Alba and Meira are certainly correct when they state that truly monodisperse synthetic polymers are impossible to obtain. However, the ability to examine *nearly* monodisperse fractions of HPSEC-separated "narrow" standards has been shown to permit the detection and quantification of secondary IB effects that are in themselves extremely small. As mentioned earlier, the applications of the technique to proteins will be the most important. The secondary broadening that occurs after the LS detection may be probed by proteins of known narrow distributions even if they are too small to confirm such mondispersity by means of measurements of the corresponding mean square radius.

ACKNOWLEDGEMENTS

The skillful experimental measurements of Lena Nilsson and Janet Howie are gratefully acknowledged. The contributions of Dr. Louis Papazian and Dr. David Shortt to the analytical interpretations presented in this paper are appreciated.

REFERENCES

1 B.H. Zimm, *J. Chem. Phys.*, 16 (1948) 1093.
2 H.C. van de Hulst, *Light Scattering by Small Particles*, Dover, New York, 1981.
3 P. Debye, *J. Phys. Colloid Chem.*, 51 (1947) 18.
4 P.F. Mijnlieff and D.J. Coumou, *J. Colloid Interface Sci.*, 27 (1968) 553.
5 P.J. Wyatt, *Anal. Chim. Acta*, 272 (1993) 1.
6 L.H. Tung, *J. Appl. Polym. Sci.*, 10 (1966) 375.
7 L.H. Tung, *J. Appl. Polym. Sci.*, 13 (1969) 775.
8 K.S. Chang and Y.M. Huang, *J. Appl. Polym. Sci.*, 16 (1972) 329.
9 T. Ishige, S.-I. Lee and A.E. Hamielec, *J. Appl. Polym. Sci.*, 15 (1971) 1607.
10 L.M. Gugliotta, J.R. Vega and G.R. Meira, *J. Liq. Chromatogr.*, 17 (1990) 1671.
11 D. Alba and G.R. Meira, *J. Liq. Chromatogr.*, 9 (1986) 1141.